Proceedings of
ASME TURBO EXPO 2002
June 3-6, 2002, Amsterdam, The Netherlands

GT-2002-30600

NUMERICAL INVESTIGATION OF THE EFFECT OF ASH PARTICLE DEPOSITION ON THE FLOW FIELD THROUGH TURBINE CASCADES

Hesham El-Batsh [1]

Institute of Thermal Turbomachines and Powerplants,
Vienna University of Technology
Getreidemarkt 9/313,
A-1060 Vienna, Austria

Hermann Haselbacher

Institute of Thermal Turbomachines and Powerplants,
Vienna University of Technology
Getreidemarkt 9/313,
A-1060 Vienna, Austria

ABSTRACT

Ash deposition on turbine blade surfaces is studied in this work using a particle deposition model. The model involves the three main processes: particle transport to the blade surface, particle sticking at the surface and particle detachment from the surface. The model is used to investigate the effect of ash particle deposition on the flow field through turbine cascades. The surface velocity and the downstream total pressure coefficient are calculated for the clean and the fouled blade profiles and used in this investigation.

The profile of the clean blade is chosen from the literature for which flow field measurements are available. The two-dimensional, compressible flow field is solved for the clean blade using the RNG k-ε turbulence model with the two-layer zonal model for the near-wall region. The results are compared to the experimental data.

The flow field is solved at the conditions expected in modern gas turbines. The deposition distribution on the blade surface is calculated during three periods of 12 operating hours each assuming inlet particle concentration as 100 $ppmw$. The fouled blade profile is predicted after each period. Then the flow field and deposition calculations are repeated to account for the time-dependent particle deposition. The flow field is calculated for the fouled blade after 36 operating hours and investigated using the experimental data and the numerical calculations of the clean blade. The profile loss of the fouled blade is also predicted and compared to that of the clean blade.

[1] Now at the Mechanical Engineering Technology Department, Banha High Institute of Technology, Banha 13512, Egypt

NOMENCLATURE

a	radius of the contact area, $[m]$
A_{cp}	area in the stream direction, $[m^2]$
c	blade chord length, $[m]$
c_{ax}	blade axial chord length, $[m]$
C	total pressure coefficient $= (p_{o2} - p_{o1})/0.5\rho_2 U_2^2$, $[-]$
$\overline{C}$	mass averaged total pressure loss coefficient, $[-]$
Cu	Cunningham correction factor, $[-]$
C_D	Drag coefficient, $[-]$
D_p	particle diameter, $[m]$
E_p	Young's modulus of particle material, $[Pa]$
E_s	Young's modulus of surface material, $[Pa]$
f	correction factor for the wall effect, $[-]$
F_D	fluid drag force, $[N]$
F_{po}	sticking force, $[N]$
F_L	fluid lift force, $[N]$
K_c	composite Young's modulus, $[Pa]$
M_{is}	isentropic exit Mach number, $[-]$
p_o	total pressure, $[Pa]$
Re_p	particle Reynolds number, $[-]$
s	distance along blade surface, $[m]$
S	blade pitch, $[m]$
u	velocity in x-direction, $[m/s]$
u_τ	wall friction velocity, $[m/s]$
$u_{\tau c}$	critical wall shear velocity, $[m/s]$
u^+	dimensionless velocity, $[-]$
u_c	velocity at the center, $[m/s]$

U	main stream velocity, $[m/s]$
W_A	work of sticking, $[J/m^2]$
x	distance in x-direction, $[m]$
y	distance in y-direction, $[m]$
y^+	dimensionless wall distance, $[-]$
α	particle deformation, $[m]$
μ	fluid viscosity, $[Pa\ s]$
ν_s	Poisson ratio of surface material, $[-]$
ν_p	Poisson ratio of particle material, $[-]$
ρ	fluid density, $[kg/m^3]$

Subscripts
1 inlet
2 exit

INTRODUCTION

Limited access to and hence high costs of high quality fuels such as natural gas and light distillates have led many operators of gas turbine installations to consider low-grade fuels. Most commonly used are crude oils and biomass. These fuels are always contaminated with varying levels of impurities. Combustion of such fuels produces large amounts of ash.

Ash particles in the hot gas stream have various effects. Impacting on turbine blade surface by their inertia they can cause erosion. When the ash particles in the hot gas stick to the blade surface, they build up layers of deposits. The aerodynamic performance deteriorates due to growing deposit thickness, decreasing the efficiency and the power of the gas turbine. Consequently, the machine has to be shut down at certain intervals for blade cleaning. Ash particle deposition on the turbine hot sections may result also in premature damage of turbine blades due to hot corrosion.

Kawagishi et al. (1992) studied the effect of particle deposition on turbine performance by using a single stage experimental turbine. In order to simulate the deposits, solids of silicone compounds were artificially attached to the nozzles and the moving blades. Location and quantity of deposits were chosen from a typical distribution of deposit in actual turbines. They found that the profile loss was strongly increased by particle deposition. They found also that particle deposition decreased the stage efficiency over a wide range of the output power by about 20%.

Bölcs and *Sari* (1988) studied experimentally the effect of deposits on the flow in a turbine cascade. They attached plastic cement on the blade surface according to a real distribution of deposits obtained from a gas turbine. They investigated the flow field of the clean blade and of the fouled blade. They found that because of the high surface roughness of the deposits, the boundary layer became turbulent and thicker almost immediately downstream of the blade leading edge on the suction surface. Obviously, the increase in the boundary layer thickness gives a thicker wake with large recirculation zones and thus high losses.

The aim of this work is to investigate the effect of ash particle deposition on the flow field through turbine cascades. In a first step, the flow field is numerically solved for the clean blade. The total pressure coefficient is calculated downstream of the cascade and compared to the experimental data. In the second step, the flow field is solved at a condition similar to the conditions in modern gas turbines. Then the time-dependent particle deposition is predicted by using a deposition model. Finally, the flow field of the fouled blade is solved. The surface velocity and the downstream total pressure coefficient of the fouled blade are compared to those of the clean blade and to the experimental data.

PARTICLE DEPOSITION MODEL

The processes governing the rate of particle deposition are: the transport of particles to the surface, the sticking of particles at the surface due to the sticking forces between the particles and the surface and the detachment of particles from the surface by the fluid flow.

Theoretical studies of particle transport can be developed either by Eulerian approach or by Lagrangian approach. The Eulerian approach is based on the assumption that two continuous fields are present and the transport equations are solved for both phases at the same time. In the Lagrangian approach, a number of particle trajectories are simulated by solving the particle equation of motion, i.e., the particles are considered individually.

The previous work showed that the Lagrangian approach provides a detailed and realistic model for particle transport. In addition, it gives the complete information on particle impact at the surface required for sticking studies. Therefore, this approach is used in this study.

Particle Transport

The particle transport model used in this work is the Lagrangian one given by *El-Batsh* and *Haselbacher* (2000). In this model, the particle trajectory is calculated by solving the particle equation of motion considering various forces applied on the particle. The eddy lifetime model is used to represent the effect of turbulent fluctuating velocity on the particle trajectory.

Particle Sticking

The probability of particle sticking to a surface is a function of several parameters including particle size, particle and surface properties, particle velocity and its angle of incidence. Previous investigations of the impact and sticking

are available in the literature for spherical particles. The coefficient of restitution is defined as the ratio of the normal rebound velocity to the normal impact velocity. *Dahneke* (1975) studied experimentally the effect of particle impact velocity on the rebound velocity for spherical particles. He found that when the particle normal impact velocities are relatively high, the coefficient of restitution is relatively constant. But, as these velocities decrease, the significance of the sticking force increases and the rebound velocities drop off considerably. Eventually, a point is reached when no rebound occurs and the particles are captured. This velocity is called the capture velocity.

Brach and *Dunn* (1992) developed a sticking model for spherical particles. They calculated the capture velocity below which no rebound occurs from the elastic properties of the particle and surface materials. This model was tuned by *El-Batsh* and *Haselbacher* (2001) to obtain conditions similar to the conditions of gas turbines when low grade fuels are used. The tuned model was based on the assumption that the surface elastic properties are those for the particles assuming a monolayer exists on the surface. In the present study, the time required to build a monolayer on the blade surface is very short in comparison to the time required to build a layer which significantly changes the flow field. Therefore, this assumption is appropriate and the model is used to simulate the sticking process.

Particle Detachment

When the removal forces from the fluid flow are sufficient to prevent the particles from remaining on the surface, the particles are detached. The deposition model is extended in this study with a particle detachment model to study the stability of the particles at the surface.

Various mechanisms of particle detachment are rolling, sliding and lifting. *Soltani* and *Ahmadi* (1994) studied these mechanisms and found that spherical particles are released from the surface by rolling rather than sliding or lifting. Therefore, particle detachment from smooth surfaces is caused by the fluid dynamic moment in the viscous sublayer. Detachment occurs when this moment exceeds the moment exerted on the particle by the sticking force.

Figure 1 shows the geometric features of a spherical particle stuck to a plane surface. The critical moment is applied to describe the mechanism of particle detachment from a surface. Accordingly, the particle is detached when external force moment about the point 'O' overcomes the resisting moment due to the sticking force, i.e.

$$F_D(\frac{D_p}{2} - \alpha) + F_L a \geq F_{po} a \tag{1}$$

In most cases of elastic particle sticking, α is very small in comparison to $D_p/2$ and could be neglected. *Soltani*

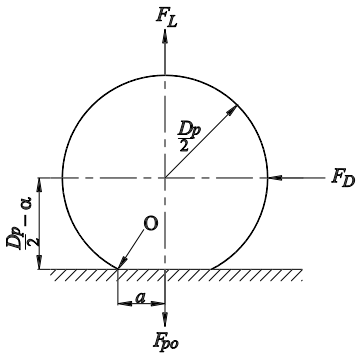

Figure 1: Geometric features of a spherical particle stuck to a smooth surface

and *Ahmadi* (1994) found that the effect of the lift force on particle detachment is negligible. Therefore, equation 1 becomes:

$$F_D \frac{D_p}{2} \geq F_{po} a \tag{2}$$

In the viscous sublayer, the dimensionless streamwise velocity is given by:

$$u^+ = y^+ \tag{3}$$

where the dimensionless quantities are defined as:

$$u^+ = \frac{u}{u_\tau}, \qquad y^+ = \frac{u_\tau y \rho}{\mu} \tag{4}$$

For smooth surfaces, the velocity component at the center of a stuck spherical particle u_c is given by:

$$\frac{u_c}{u_\tau} = \frac{u_\tau D_p \rho}{2\mu} \tag{5}$$

or

$$u_c = \frac{D_p \rho}{2\mu} u_\tau^2 \tag{6}$$

The drag force acting on a spherical particle is given by:

$$F_D = \frac{1}{2} C_D \rho u_c^2 A_{cp} f / Cu \tag{7}$$

where $A_{cp} = (\pi/4) D_p^2$ is the area in the stream direction, Cu is the Cunningham correction factor and f is the correction factor for the wall effect given by *Soltani* and *Ahmadi* (1994) as 1.7.

For small particles, the Reynolds number is quite small and the Stokes drag may be used.

$$C_D = \frac{24}{Re_p}, \qquad Re_p = \frac{D_p \rho u_c}{\mu} \tag{8}$$

Then, the drag force is given by:

$$F_D = \frac{3\pi f \mu D_p}{Cu} u_c \tag{9}$$

From equation 6

$$F_D = \frac{3\pi f}{2Cu} D_p^2 \rho u_\tau^2 \tag{10}$$

The radius a of the contact area can be calculated from the relation given by *Soltani* and *Ahmadi* (1994) and *Rimai et al.* (1994) as:

$$a = \left(\frac{3\pi W_A D_p^2}{2K_c} \right)^{\frac{1}{3}} \tag{11}$$

where K_c is the composite Young's modulus given by:

$$K_c = \frac{4}{3} \left[\frac{(1-\nu_s^2)}{E_s} + \frac{(1-\nu_p^2)}{E_p} \right]^{-1} \tag{12}$$

and the work of sticking W_A is a constant which depends upon the material properties of the particle and the surface and has the units of J/m^2. This constant is obtained experimentally.

The sticking force F_{po} is calculated as given by *Soltani* and *Ahmadi* (1994) and *Rimai et al.* (1994) as:

$$F_{po} = \frac{3}{4}\pi W_A D_p \tag{13}$$

Substituting from equations 10, 11 and 13 in equation 2 leads to the relation for the critical wall shear velocity:

$$u_{\tau c}^2 = \frac{CuW_A}{\rho D_p} \left(\frac{W_A}{D_p K_c} \right)^{\frac{1}{3}} \tag{14}$$

Therefore, the particle is removed from the surface if the turbulent flow stream has a wall friction velocity which is higher than $u_{\tau c}$.

Equation 14 is based on the material properties of the particle and the surface. These properties are not available in the literature for ash. The elastic properties presented by *Soltani* and *Ahmadi* (1994) and *Brach* and *Dunn* (1992) for various types of particles showed that the Poisson ratio changed from 0.27 to 0.33 while the Young's modulus changed by several orders of magnitude. According to equation 12, the Young's modulus has the major effect on particle detachment in this range of Poisson ratio. It has also the major effect on particle sticking as found by *El-Batsh* (2001). Therefore, the Young's modulus of ash particles was measured at the *Department of Materials Science and Testing, Vienna University of Technology*. The measured value was 18.4×10^9 Pa. The particle Poisson ratio was considered as 0.27. To obtain the surface material properties, it was assumed that a monolayer exists on the surface as discussed above. Therefore, the surface material properties had the same values of those for ash particles. Finally, the work of sticking is not available in the literature for ash particles and could not be measured in this study. The available value for Silicon particles ($W_A = 0.039$ J/m^2) as given by *Soltani* and *Ahmadi* (1994) is used.

The commercial CFD code Fluent is used to calculate particle trajectories. A user-defined subroutine is employed to model the particle-wall interaction. In this subroutine, the sticking and the detachment models are implemented.

MODELING FLOW FIELD

The flow field is modeled by solving the governing equations for fluid flow and heat transfer. The time averaging procedure known as Reynolds averaging is used to obtain the conservation equations for turbulent flows. An eddy-viscosity model is employed in which the Reynolds stresses are assumed to be proportional to the mean velocity gradient with the constant of proportionality being the turbulent viscosity. The results of *El-Batsh* and *Haselbacher* (2000) showed that the Renormalization Group (RNG) k-ε model is an appropriate turbulence model for particle deposition. Therefore, this model is used in the present study with the near-wall region solved by the two-layer zonal approach. The surface of the clean blade and that of the fouled blade are assumed smooth. Further study is required to investigate the effect of surface roughness on the flow field. The flow field is calculated in Fluent using Quadratic Upwind Interpolation (QUICK).

PERFORMANCE OF THE CLEAN BLADE

The von Karman Institute (VKI) transonic inlet turbine guide vane was employed in this study with the experimental measurements of *Arts et al.* (1990). The aerodynamic performance of the blade is investigated using the surface velocity and downstream total pressure coefficient.

Flow Field Numerical Calculations

Computational Grid: A two-dimensional structured grid with total number of cells of about 19000 was used in this study. The inlet plane was chosen at a distance of 1.35 axial chord ahead of the blade leading edge. The downstream boundary was at 1.16 axial chord behind the blade trailing edge. Figure 2 shows the grid near the blade leading and trailing edges. The distance between the wall and the adjacent cells was chosen to satisfy the limits of the dimensionless wall distance y^+.

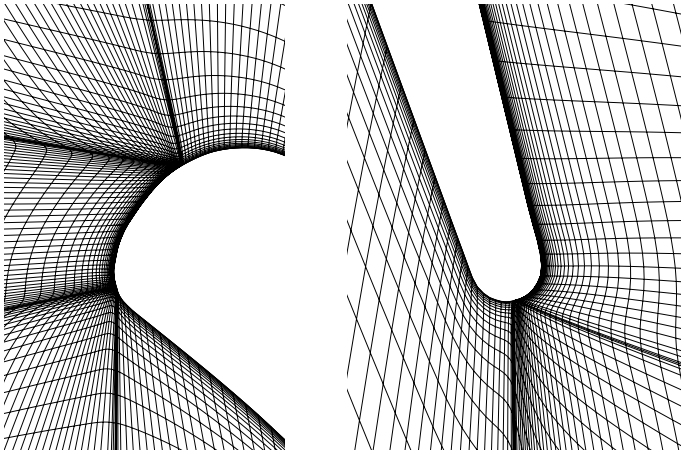

Figure 2: Computational grid near the blade leading and trailing edges

Numerical Calculations: The compressible flow field was solved for two isentropic exit Mach numbers M_{is} corresponding to the experiments. The total pressure was used to define the fluid condition at the inlet while the static pressure was employed at the exit. The flow field was calculated at $M_{is} = 0.875$ to compare the surface velocity with the experimental data. The solution at $M_{is} = 0.85$ was employed to predict the profile loss and to compare the downstream total pressure with the experimental data.

Grid Sensitivity Study

Hildebrandt and *Fottner* (1999) studied the effect of grid refinement on the flow field through turbine cascades. They found that a grid independent solution could be obtained with a number of cells in the order of 12000 cells. Based on their result, using the previous grid with 19000 cells would satisfy the grid independent solution. To confirm the independent solution, the grid density was increased in both directions by 20 %. The two grids with 19000 and 27000 cells were employed in the grid sensitivity study. For both grids, the dimensionless wall distance y^+ near the wall was smaller than 3. The downstream total pressure coefficient C was used in the study. It is defined as:

$$C = \frac{p_{o2} - p_{o1}}{0.5\rho_2 U_2^2} \tag{15}$$

where p_{o1} is total inlet pressure, p_{o2} is total exit pressure, U_2 is the exit velocity and ρ_2 is the exit density.

Figure 3 shows the comparison between the pitchwise variation of the total pressure coefficient calculated using both grids and the experimental data. For clarity of presentation, the location of minimum pressure was taken as the origin. The figure shows that the numerical calculations agree well with the experimental data. The discrepancy is caused by the fully turbulent model used in the calculations. This model overestimated the profile loss resulting in a wide and deep wake. More accurate calculations could be obtained by using a model which can predict the laminar and the transition regions. The comparison between the calculations performed using both grids confirmed that the solution was grid independent.

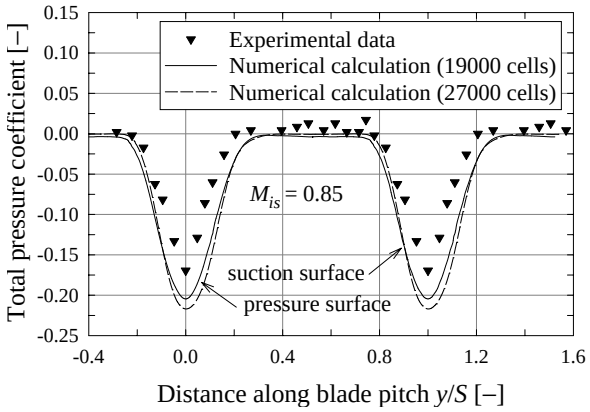

Figure 3: Pitchwise variation of the total pressure coefficient

ASH PARTICLE DEPOSITION ON TURBINE BLADES

The deposition calculations performed in this study were based on the assumption that the temperature in the entire computational domain including the thermal boundary layer and the blade surface is higher than the dew point of the alkali components. In addition, it is lower than the softening temperature of the ash. Therefore, particle sticking is based on the elastic properties of particle and surface materials.

Flow Field Numerical Calculation

The compressible flow field was solved for the isentropic exit Mach number of 0.875. The inlet temperature was chosen as 1500 K to represent a typical inlet gas temperature in gas turbines. For a first estimate, the surface temperature distribution was obtained from the literature. The distribution was at midspan for a cooled blade operating at the inlet gas temperature mentioned above as given by *Cohen et al.* (1987). The temperature versus the dimensionless axial distance x/c_{ax} was determined from the typical temperature distribution. Then, the temperature was applied on the

VKI transonic guide vane as shown in figure 4. More accurate calculations need to consider the internal heat transfer inside the blades. Table 1 summarizes the boundary conditions used for this study.

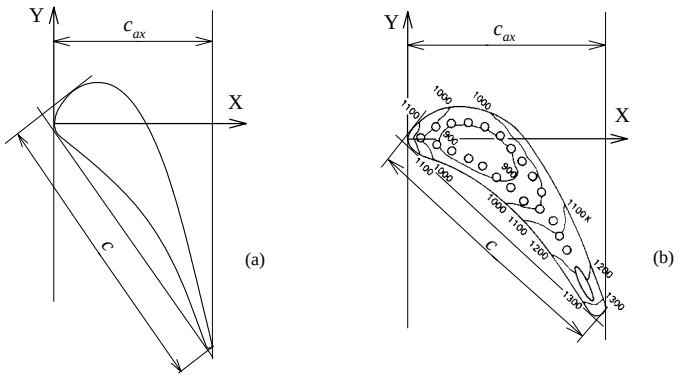

Figure 4: (a) The VKI transonic inlet guide vane, (b) Temperature distribution at midspan, *Cohen et al.* (1987)

Isentropic exit Mach number, [–]	0.875
Total inlet pressure, $[Pa]$	147500
Total inlet temperature, $[K]$	1500
Free stream turbulence, [%]	1
Static outlet pressure, $[Pa]$	89600
Wall temperature, $[K]$	1000-1300

Table 1: Flow field boundary conditions prior to deposition calculations

Particle Specifications and Boundary Conditions

Extensive review of the previous measurements on ash particle properties and size distributions by *El-Batsh* (2001) showed that the ash particles produced from the combustion of low-grade fuels are in the size range from 0.25 μm to 20 μm. It showed also that cyclone separators can efficiently remove the particles in the size range of $>$ 5-10 μm. Therefore, using the cyclone separators, the majority of the particles after the cyclone will be smaller than 5 μm. The review indicated also that uncontrolled ash loading (without cleaning systems) is expected to be in the 200-300 $ppmw$ range and the cyclone separators can reduce the ash loading in the turbine gas part by a factor of about two. Based on this review, the particle specifications at the inlet to the cascade were assumed in this study as given in table 2.

Particle size distribution, $[\mu m]$	0.25-5
Particle concentration, $[ppmw]$	100
Particle density, $[kg/m^3]$	1700

Table 2: Assumed particle specifications at the inlet to the cascade

Deposition Numerical Calculations

Hamrick and *Schiefelbein* (1991) presented the results of a program to develop biomass as an alternative fuel for gas turbines. The results indicated that after approximately 26 hours of operation the gas turbine power output started to decline due to deposition, and the gas turbine was cleaned. Based on this result, it was decided to calculate particle deposition in 36 operating hours and to predict the blade performance after this period. This period was divided into three calculation periods of 12 hours each. These three time steps were chosen to solve the time-dependent particle deposition and to compromise between computational time and accuracy. It was assumed that the flow field was time independent during the calculation period.

To calculate particle deposition in each period, a sample of 13183 particles was used with the peak in the mass distribution at 2 μm. The particles were uniformally distributed over the blade pitch and were injected with velocities and temperatures equal to the fluid inlet velocity and temperature, respectively. Then the particle trajectories were calculated. Each particle trajectory was calculated 100 times to account for the effect of turbulence on the particle trajectory and to build a deposition layer on the surface.

The sticking model was applied for the impacted particles at the surface by calculating the particle capture velocity. The detachment model was applied on the stuck particles at the surface by comparing the critical wall shear velocity with the fluid wall friction velocity. The rebounded and detached particles continued the trajectory until they left the domain or impacted the blade surface in another place.

Particle deposition distribution on the VKI transonic inlet guide vane was calculated after 12 operating hours by calculating the deposition from the injected sample of particles. Then, the results were simply multiplied by a factor corresponding to the mentioned period and inlet particle concentration.

The fouled blade profile was predicted using deposition data assuming that the deposit density equals to 0.7 of the particle material density.

The compressible flow field was solved for the fouled profile after 12 hours by using the same boundary conditions given in table 1. The change in heat transfer caused by the deposits was not considered. The increase in surface rough-

ness due to particle deposition was not considered either. Further investigations are required to study the effect of these parameters on the flow field and on the mass rate of deposition. The deposition calculations were performed for the second period. Then the flow field and the deposition calculations were repeated for the last period.

Figure 5 shows the deposition distributions in the three periods. The origin here represents the theoretical stagnation point of the fouled blade which is determined as the blade point with the minimum axial distance. The figure shows that the maximum deposition in all periods occurred on the blade pressure surface. A small amount of deposition was predicted on the blade suction surface. Most of the particles were reaching the surface by the effect of inertia force because they were supermicron particles. The figure indicates that the deposition distribution depended upon the profile of the fouled blade. The location at which the maximum deposition occurred moved toward the stagnation point with time. The maximum deposition thickness calculated in each period was smaller than the maximum thickness calculated in the previous period.

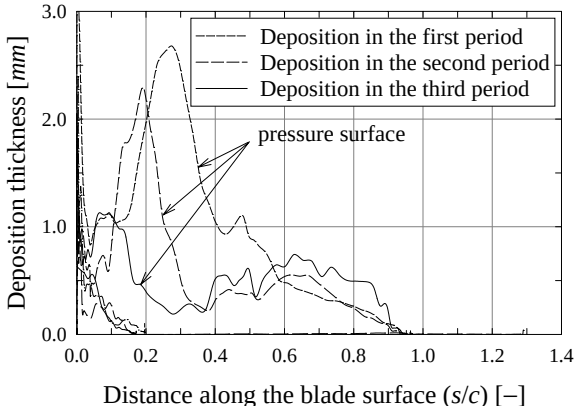

Figure 5: Predicted deposition thickness distribution in three calculation periods

PERFORMANCE OF THE FOULED BLADES

Figure 6 shows the predicted profile of the fouled blade after each period. The deposition model predicted a thick layer on the blade pressure surface and on the blade leading edge.

A two-dimensional structured grid was generated with about 18000 cells. The compressible flow field was solved for the isentropic exit Mach number of 0.875 using the RNG k-ε model with the two-layer zonal model.

Figure 7 shows the distribution of the surface velocity of the clean blade and that of the fouled blade after 36 operating hours. The figure indicates that in the case of the clean blade, the acceleration of the flow was smooth on both the suction surface and the pressure surface. For the fouled blade profile, the flow acceleration was not smooth on the pressure surface. There was a zone of decelerating flow at about 90 % of the chord where the flow separation might occur resulting in increased profile loss. The small wiggle on the suction surface close to the trailing edge was caused by the numerical solver.

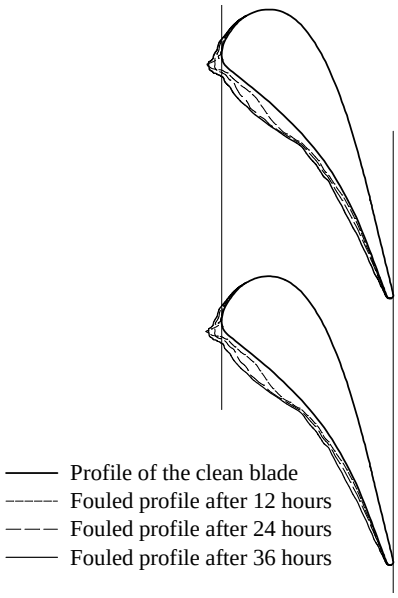

Figure 6: Predicted fouled blade profile after 36 hours

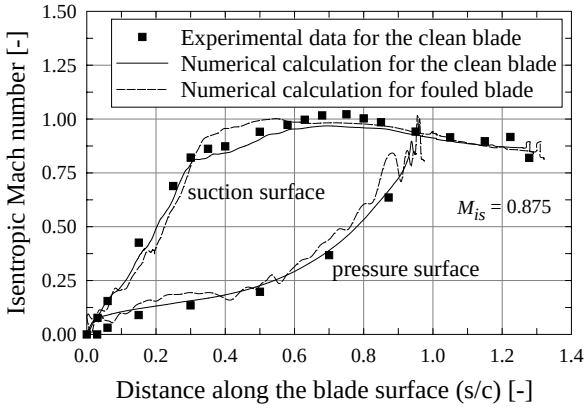

Figure 7: Surface velocity distribution of the fouled blade after 36 operating hours

The flow field was solved also for the isentropic exit Mach number of 0.85. The total pressure coefficient was calculated using equation 15. Figure 8 shows the comparison between the total pressure coefficient for the fouled blade after 12 hours and 36 hours. The figure shows also the calculated

total pressure coefficient and the experimental data of the clean blade. The figure indicates that the downstream total pressure decreased for the fouled blade. The decrease in the total pressure after 36 hours was higher than that after 12 hours. For the fouled profiles after 12 and 36 hours, the reduction in the total pressure was higher than the reduction in the total pressure for the clean blade profile.

The mass averaged total pressure loss coefficient $\overline{C}$ was calculated from

$$\overline{C} = -\frac{\int_0^S C\rho u \; dy}{\int_0^S \rho u \; dy} \tag{16}$$

Figure 9 shows the mass averaged total pressure loss coefficient versus time. The figure indicates that the profile loss increased by about 60% after 36 operating hours.

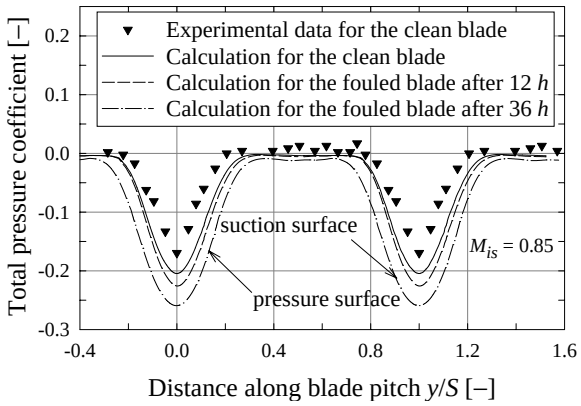

Figure 8: Predicted total pressure coefficient for the fouled blade after 36 hours

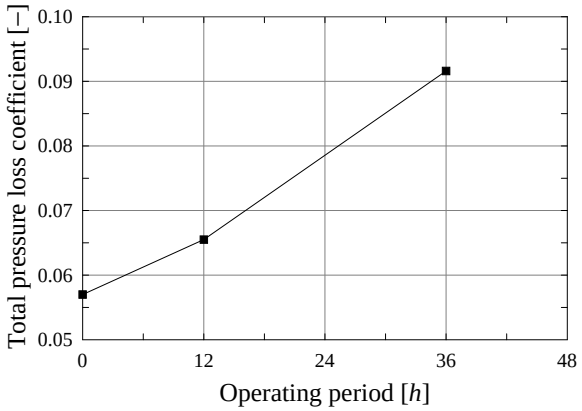

Figure 9: Mass averaged total pressure loss coefficient

CONCLUSIONS

In this study, a particle deposition model was used to investigate the effect of ash particle deposition on the performance of turbine blades. A blade profile was chosen from the literature and the time-dependent particle deposition was calculated in 36 operating hours. Based on the results obtained for this blade profile and for the particle size distribution assumed in this study, it was found that:

- The maximum deposition occurred on the blade pressure surface. The location of the maximum deposition moved towards the stagnation point as the operating time increased.
- The investigation of the surface velocity for the fouled blade showed that the flow acceleration was not smooth on the pressure surface. A zone of decelerating flow was predicted where the flow separation might occur resulting in increased profile loss.
- The model predicted an increase in the profile loss for the fouled blade after 36 operating hours of about 60% of that calculated for the clean blade.

ACKNO WLEDGEMENTS

The financial support from the Austrian Academic Exchange Service (ÖAD), the mission department of the Egyptian Ministry of High Education and the Austrian Science Fund (FWF) is acknowledged with thanks.

REFERENCES

Arts, T.; *De Rouvroit, M. L.* and *Rutherford, A. W.* (1990), Aero-thermal Investigation of a Highly Loaded Transonic Linear Turbine Guide Vane Cascade, VKI Technical Note 174.

Bölcs, A. and *Sari, O.* (1988), Influence of Deposit on the Flow in a Turbine Cascade, ASME paper 88-GT-207.

Brach, R. and *Dunn, P.* (1992), A Mathematical Model of the Impact and Adhesion of Microspheres, Aerosol Science and Technology, Vol. 16, No. 1, 51-64.

Cohen H.; *Rogers, G. F. C.* and *Saravanamuttoo, H. I. H.* (1987), Gas Turbine Theory, Longman Scientific & Technical.

Dahneke, B. (1975), Further Measurements of the Bouncing of Small Latex Spheres, Journal of Colloid and Interface Science, Vol. 51, No. 1, pp. 58-65.

El-Batsh, H. and *Haselbacher, H.* (2000), Effect of Turbulence Modeling on Particle Dispersion and Deposition on Turbine Blades, ASME paper, 2000-GT-519.

El-Batsh, H. and *Haselbacher, H.* (2001), Effect of Gas and Surface Temperatures on Particle Deposition on Turbine Blades, Fourth European Conference on Turbomachinery, 21-23 March, Florence, Italy.

El-Batsh, H. (2001), Modeling Particle Deposition on Compressor and Turbine Blade Surfaces, Ph.D. Thesis, Vienna University of Technology, Vienna, Austria.

Hamrick, J. T. and *Schiefelbein, G. F.* (1991), Development of Biomass as an Alternative Fuel for Gas Turbines, Pacific Northwest Laboratory, Richland, W ashington 99352, PNL-7673, DE91 012129.

Hildebrandt, T. and *Fottner, F.* (1999), A Numerical Study of the Influence of Grid Refinement and Turbulence Modeling on the Flow Field Inside a Highly Loaded Turbine Cascade, Journal of Turbomachinery, October 1999, Vol. 121, pp. 709-716.

Kawagishi, H.; *Nagao, S.* and *Kawasaki, S.* (1992), Performance Evaluation of Geothermal Steam Turbine with Scale Deposits, PWR-Vol. 18, Steam Turbine-Generator Developments for the Power Generation Industry, ASME, pp. 69-73.

Rimai, D. S.; *Demejo, L. P.* and *Bowen, R. C.* (1994), Mechanics of Particle Adhesion, J. Adhesion Science Technology, Vol. 8, No. 11, pp. 1333-1355.

Soltani, M. and *Ahmadi, G.* (1994), On Particle Adhesion and Removal Mechanisms in Turbulent Flows, J. Adhesion Science Technology, Vol. 8, No. 7, pp. 763-785.